JOURNAL OF APPLIED ELECTROCHEMISTRY 24 (1994) 713–718

Mechanism of the reverse dissolution of zinc in the presence of nickel
Part II: Influence of triethylbenzylammonium chloride

C. CACHET, R. WIART

UPR 15 du CNRS, Physique des Liquides et Electrochimie, Laboratoire de l'Université Pierre et Marie Curie, Tour 22, 4 Place Jussieu, 75252 Paris, Cedex 05

I. IVANOV, Y. STEFANOV, S. RASHKOV

Institute of Physical Chemistry, Bulgarian Academy of Sciences, Sofia 1040, Bulgaria

Received 20 December 1993; revised 28 January 1994

Cyclic voltammetry and impedance measurements were used to investigate the influence of an additive, triethyl-benzyl-ammonium chloride, on the kinetics of zinc deposition in acidic sulphate electrolytes containing Ni^{2+} ions able to induce the reverse dissolution of zinc deposits. It is shown that the adsorbed additive inhibits both the nucleation and growth of zinc deposits. By competing with the formation of a nickel-containing surface compound responsible for a stimulation of hydrogen evolution, the additive adsorption also inhibits hydrogen evolution and thereby stabilizes the galvanostatic deposition of zinc.

1. Introduction

The processes involved in zinc electrodeposition are highly sensitive to the presence of organic or mineral impurities [1] either added to the electrolyte or possibly generated during the electrolysis.

In highly acidic sulphate electrolytes, the kinetics of zinc deposition have been extensively investigated on the basis of electron microscopy, cyclic voltammetry and current efficiency [2–6]. It is known that the hydrogen discharge reaction is inhibited by the presence of Zn^{2+} ions in the electrolyte, and activated by the presence of nickel impurities in the electrolyte.

From impedance measurements and potentiostatic polarization curves, it has been shown that zinc deposition normally occurs when hydrogen evolution is passivated on the deposit surface [7, 8]. Then the depassivation process is facilitated by the presence of nickel impurities in the electrolyte, leading to the deposit redissolution. By using a separator between the cathode and the platinum anode compartments, it has been recently shown that the deleterious influence of Ni^{2+} ions is enhanced by the anodically formed products which interfere with the interfacial processes taking place at the cathode surface [9].

In the electrolytes for zinc electrowinning, organic compounds are generally added to control the adverse effect of metal impurities on the efficiency [3, 10–15]. Generally, they influence the zinc electrode polarization and they modify the morphology and preferred orientation of zinc deposits. The beneficial effect of triethyl-benzyl-ammonium chloride (TEBA) in nickel-containing electrolytes has been related to a decrease in the screening effect of hydrogen bubbles where local galvanic cells can be generated [14–16]. This additive has been shown to increase the induction period which precedes the reverse dissolution of zinc deposits obtained under galvanostatic conditions in nickel-containing electrolytes [17].

The present work is particularly devoted to the influence of TEBA on the kinetics of zinc deposition and reverse dissolution of zinc deposits.

2. Experimental details

Experimental details have been described previously [9]. The electrolysis cell was thermostated at 38° C. A Nafion® diaphragm (Dupont de Nemours) was used to separate the anode from cathode; the cathode and the reference electrode (saturated mercury sulphate electrode, SSE) were placed in the same compartment. The counter electrode was a platinum gauze cylinder. Two different cathodes were used, whose effective surfaces were vertically oriented in the cell: (i) a pure aluminium cathode (Johnson–Matthey, specpure) insulated with epoxide resin and (ii) a sheet of aluminium supplied by Riedel de Haën (RdH, purity about 99.6%) with iron content 0.2% as main impurity [6]. Before electrolysis, the effective surface of the cathode was polished with emery paper (grit 1200).

The base electrolyte consisted of 55 g dm^{-3} zinc from $ZnSO_4 \cdot 7H_2O$ and 120 g dm^{-3} H_2SO_4. To this solution, nickel was added as $NiSO_4 \cdot 6H_2O$ between 5 and 30 mg dm^{-3}, and triethyl-benzyl-ammonium chloride (TEBA) at concentrations between 0.1 and

0021-891X

$0.6\,g\,dm^{-3}$. All chemicals were Merck products of analytical grade purity, except for TEBA which was from Fluka (purity > 98%).

Impedance measurements were performed using a frequency response analyser (Solartron 1250) and an electrochemical interface (Solartron 1286) controlled by an IBM PS/2 microcomputer.

3. Results and discussion

3.1. *Voltammetry*

The influence of the organic additive TEBA in the presence of Ni^{2+} ions appears on voltammograms recorded at the beginning of electrolysis. Starting from $U = -1\,V$ stabilized voltammograms were obtained in the whole potential range, at the 7th scan.

With the pure aluminium cathode, as shown in Fig. 1, a clear inhibition of zinc deposition is generated by the organic additive, with a subsequent decrease in the peak for the deposit dissolution. It can be concluded that the additive adsorption inhibits the nucleation and growth of zinc nuclei on the aluminium substrate. It also appears in Fig. 1 that the peak observed at $-1.34\,V$, on the reverse scan without any organic additive, is practically eliminated in the presence of TEBA. Such a peak, which only appears on the reverse scan, has been ascribed to hydrogen evolution on a Ni/Zn-containing phase [4] formed at the beginning of zinc deposition on the aluminium substrate and more difficult to dissolve anodically than the rest of the zinc deposit. With the adsorption of TEBA, no peak appears, due to either the inhibition of hydrogen evolution on this phase or hindered formation of this phase.

Under the same potential sweep conditions, a similar influence of TEBA has been observed with the RdH-Al cathode, as shown in Fig. 2. However, the presence of iron impurities on the electrode surface stimulates hydrogen evolution in the absence of organic additive [6]. The peak at $-1.34\,V$, which appears on the reverse scan, is higher than for the pure aluminium substrate, and the direct scan reveals

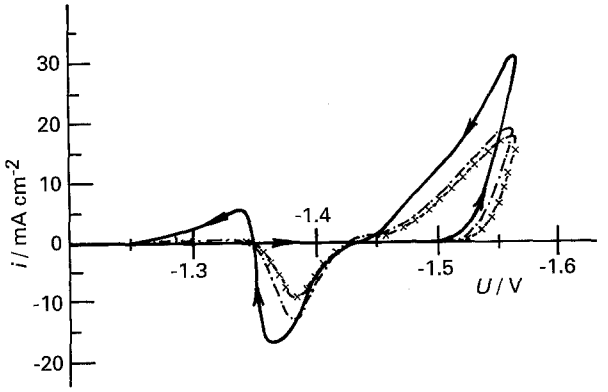

Fig. 1. Voltammograms recorded at the sweep rate $3\,mV\,s^{-1}$ on a freshly polished cathode of pure aluminium. Base electrolyte containing $5\,mg\,dm^{-3}$ Ni^{2+} (——). Influence of the TEBA concentration: $0.1\,g\,dm^{-3}$) (— · —) and $0.6\,g\,dm^{-3}$ (× — ×).

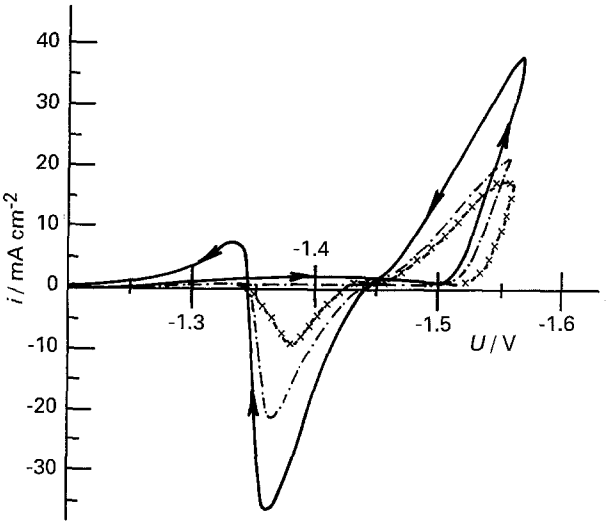

Fig. 2. Voltammograms recorded at the sweep rate $3\,mV\,s^{-1}$ on a freshly polished cathode of RdH–Al. Base electrolye containing $5\,mg\,dm^{-3}$ Ni^{2+} (——). Influence of the TEBA concentration: $0.1\,g\,dm^{-3}$ (— · —) and $0.6\,g\,dm^{-3}$ (× — ×).

a flattened peak around $-1.4\,V$. It clearly appears in Fig. 2 that both peaks are eliminated with the presence of TEBA.

3.2. *Electrode kinetics under steady-state*

The influence of TEBA on the growth of thick deposits has been investigated from steady-state measurements performed with the following procedure. First, zinc was deposited on the pure aluminium substrate during 15 min at the potential $U = -1.56\,V$, so as to form approximately a $5\,\mu m$ thick predeposit. Then the potential was pulsed to $U = -1.62\,V$ where, after stabilization of current for 10 min, a first impedance spectrum was measured. Then the cathode polarization was decreased by potential steps of 5 or 10 mV amplitude and, for each potential, the same current stabilization and impedance measurement were carried out. This procedure was automatically realized by using the software FRACOM.

3.2.1. Polarization curves. The steady-state polarization curves i/E, where E is the electrode potential corrected for ohmic drop, are shown in Fig. 3. At potentials lower than $-1.45\,V$, a clear inhibition of the electrodeposition process is produced by the organic additive TEBA. Also the peak observed between -1.35 and $-1.45\,V$ is slightly inhibited by the additive. This peak is similar to the peak observed on voltammograms and it corresponds to hydrogen evolution stimulated on the Ni/Zn-containing adsorbed species which progressively accumulates on the deposit surface when the zinc dissolution is activated with decreasing electrode polarization. Finally, at the end of zinc dissolution, the dissolution of the Ni/Zn-containing species takes place, and the current for hydrogen evolution disappears for E close to $-1.35\,V$. At this stage, it is noticeable that a subsequent increase in the cathode

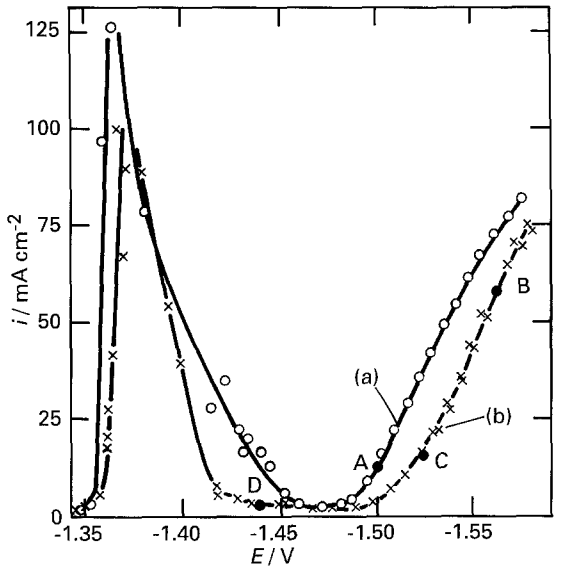

Fig. 3. Polarization curves i/E corrected for ohmic drop. (a) Base electrolyte containing 5 mg dm^{-3} Ni^{2+}. (b) With addition of 0.6 g dm^{-3} TEBA.

polarization generates no hydrogen peak, but only the curve characteristic of zinc deposition at potentials lower than −1.45 V.

The polarization curves of Fig. 3 are similar, in shape, to those already obtained without a diaphragm in electrolytes containing Ni^{2+} ions and/or H_2O_2 molecules [7, 8], where the hydrogen peak appeared at potentials of about −1.45 V. So it appears that the Ni/Zn-containing species, which generate the hydrogen peak in Fig. 3, probably behave similarly to the oxidized adsorbates (ZnO_{ad} or $ZnOH_{ad}$) involved in the reaction model previously published [8]. The presence of TEBA probably changes the kinetic parameters of this reaction model.

3.2.2. Impedance plots. The influence of TEBA on the electrode impedance is exemplified in Fig. 4. Without the additive, only one induction loop appears on plot (A) in the low-frequency domain, with a characteristic

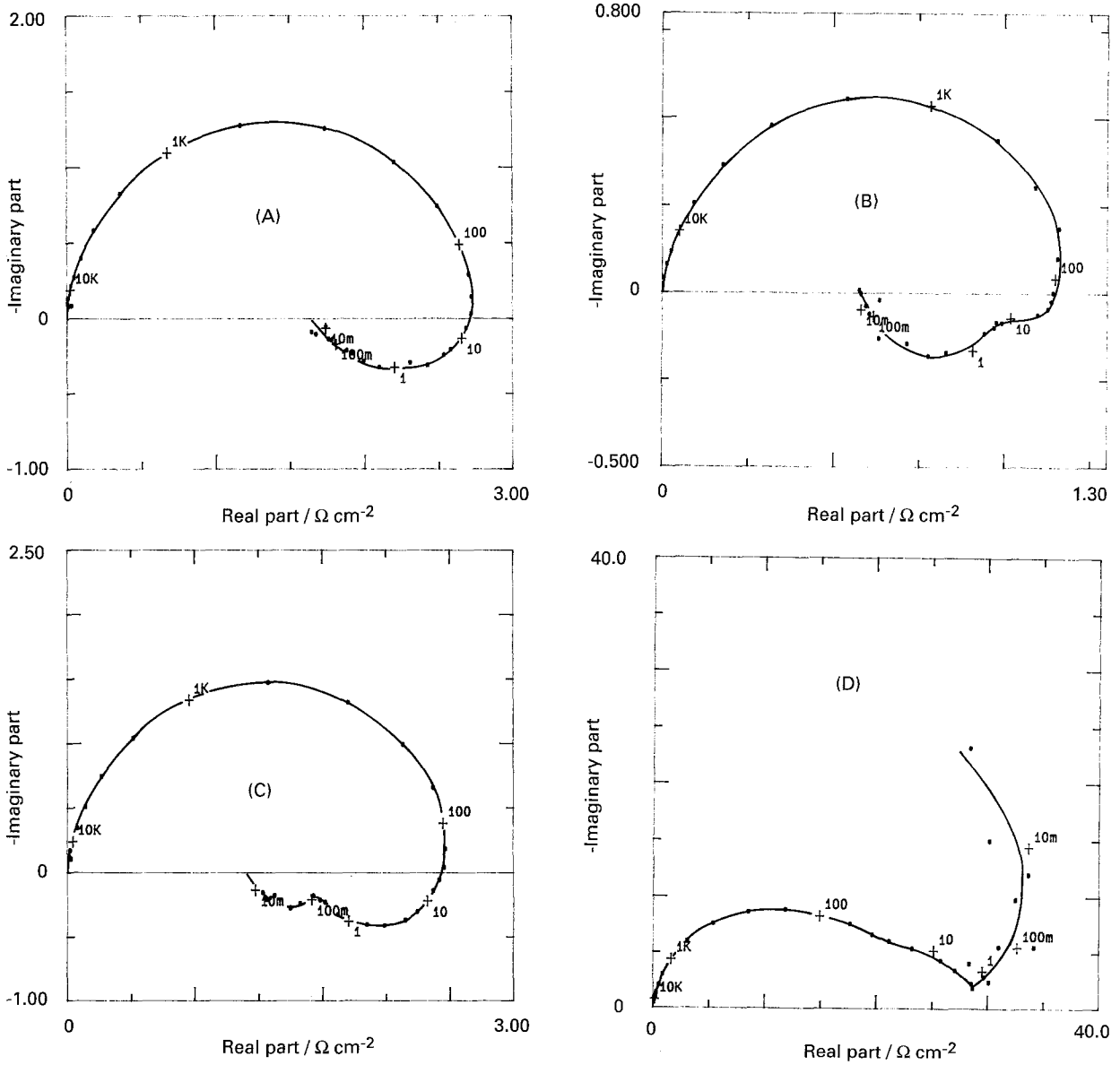

Fig. 4. Complex plane impedance plots obtained without TEBA (A) and with 0.6 g dm^{-3} (B, C and D), at points A, B, C and D in Fig. 3. (A) $E = -1.500$ V, $i = 12$ mA cm^{-2}; (B) $E = -1.562$ V, $i = 57$ mA cm^{-2}; (C) $E = -1.522$ V, $i = 17$ mA cm^{-2}; (D) $E = -1.438$ V, $i = 3.2$ mA cm^{-2}.

frequency of 1 Hz. With the presence of TEBA, two inductive loops are well separated on plots (B) and (C). With decreasing current, the proper frequencies of these two loops decrease and their respective sizes change to the benefit of the medium-frequency loop which develops. Comparing the complex plane impedance plots (A) and (C) suggests that the low-frequency inductive loop results from the presence of TEBA. With increasing current, this loop probably reflects either the slow desorption of TEBA, or a stimulated increase in the number of active sites for zinc deposition, whose renewal must be governed by the slow adsorption/desorption process of additive molecules.

At potentials where the slope of the polarization curve is negative, the impedance plots obtained with TEBA (e.g. plot D) are similar to those previously reported in additive-free electrolytes [7, 8]. The presence of several low-frequency loops confirms that several adsorbates participate in the passivation process of hydrogen evolution.

The high-frequency capacitive loop, corresponding to the double layer capacitance, C, in parallel with the charge transfer resistance, R_t, is also modified by the additive.

3.2.3. Charge transfer resistance. The potential dependence of the product of the charge transfer resistance (R_t) and current density (i) is shown in Fig. 5. It appears that this product is systematically increased in the presence of TEBA. Consequently, not only does the additive decrease the current (Fig. 3), but it increases R_t sufficiently to produce an increase in $R_t i$. This situation indicates that the activation coefficients of the electrochemical charge transfer reactions involved in both zinc deposition and hydrogen evolution on the nickel-containing adsorbed species are decreased with the adsorption of TEBA on the electrode. Only the electrochemical process taking place on the aluminium substrate at potentials close to −1.35 V is not sensitive to the presence of the additive.

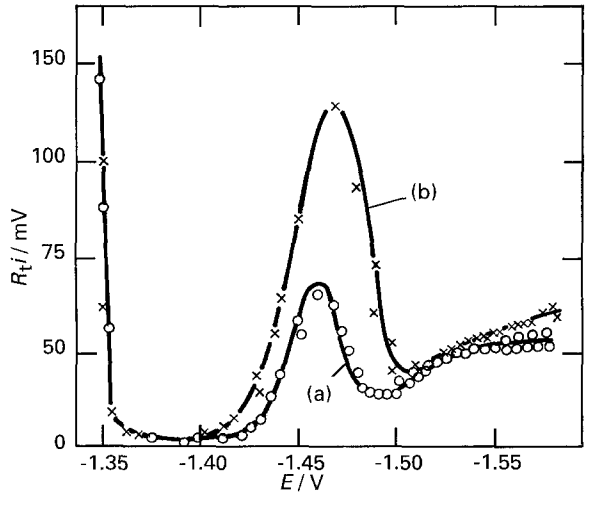

Fig. 5. Potential dependence of the $R_t i$ product. (a) Base electrolyte containing 5 mg dm^{-3} Ni^{2+}. (b) With addition of 0.6 g dm^{-3} TEBA.

3.2.4. Double layer capacitance. The double layer capacitance C of the electrode strongly depends on the electrode potential, as shown in Fig. 6. With decreasing electrode polarization from $E = -1.58$ V, in the additive-free electrolyte (curve (a)), C increases up to a maximum of 100 μF cm^{-2}, then decreases down to a minimum of 80 μF cm^{-2} and finally increases and exceeds 250 μF cm^{-2}. The initial increase is probably due to a developing roughness of the zinc surface with increasing deposition time. The decrease which follows might be due to hydrogen adsorption and/or hydrogen bubbles attached to the electrode and producing a screening effect. The final increase probably corresponds to roughening of the electrode consequent on zinc corrosion, which accompanies hydrogen evolution. On curve (b), it appears that the adsorption of TEBA predominates and decreases the capacitance over a wide potential domain (−1.40 to −1.54 V). Between −1.54 V and −1.58 V, the electrode capacitance is higher in the presence of TEBA: this is probably related to the higher roughness of the initial deposit formed at −1.58 V. Figure 7 shows that the deposit morphology is modified by adsorbed TEBA. The grains are larger, with hexagonal platelets parallel to the substrate in the additive-free electrolyte (photo A). The additive adsorption yields smaller grains of modified orientation and shape (photo B), whose total surface area may be higher than in the absence of additive. When the deposit totally disappears by dissolution at potentials close to −1.35 V, the capacitance tends towards a value of about 20 μF cm^{-2} which characterizes the aluminium substrate.

3.2.5. Influence of deposition time. Under galvanostatic conditions, the electrode impedance slowly varies with deposition time, as illustrated in

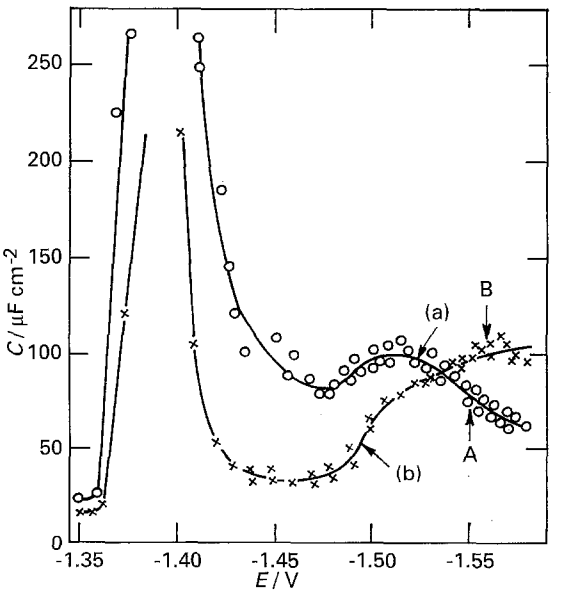

Fig. 6. Potential dependence of the double layer capacitance. (a) Base electrolyte containing 5 mg dm^{-3} Ni^{2+}. (b) With addition of 0.6 g dm^{-3} TEBA.

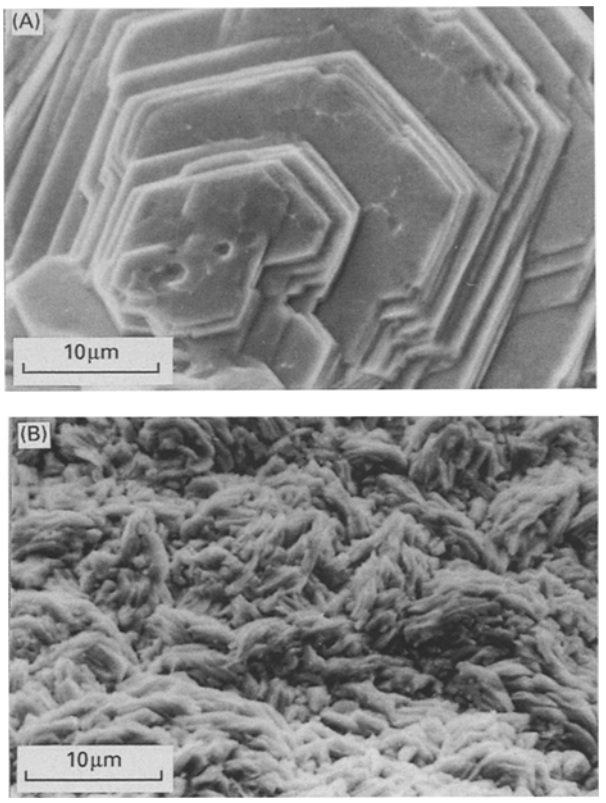

Fig. 7. Morphology of deposits obtained at points A and B in Fig. 6. (A) Without TEBA, $E = -1.550$ V, $C = 76\,\mu F\,cm^{-2}$. (B) With $0.6\,g\,dm^{-3}$ TEBA, $E = -1.557$ V, $C = 100\,\mu F\,cm^{-2}$.

Fig. 8 where the two plots have been obtained at $i = 50\,mA\,cm^{-2}$, in the presence of $0.6\,g\,dm^{-3}$ TEBA. It can be seen that passing from plot (a) to plot (b), R_t decreases from 1.25 to $1\,\Omega cm^2$, thus changing the $R_t i$ product from 62 to 50 mV. This is in agreement with Fig. 5, curve (b), since the electrode potential, E, varies from -1.55 to -1.526 V. The change in the respective sizes of the inductive loop on plots (a) and (b) also agrees with this electrode potential shift. The influence of deposition time essentially corresponds to an increase in the electrode surface area, as confirmed by the double layer capacitance, which rises from 90 to $180\,\mu F\,cm^{-2}$.

Under the same galvanostatic conditions, it has been shown [17] that the presence of TEBA in the Ni^{2+}-containing electrolyte stabilizes the formation of zinc deposits by increasing the induction period preceding zinc redissolution. The beneficial effect of the adsorbed additive is probably connected to the inhibition of both zinc deposition and hydrogen evolution on the Ni/Zn-containing adsorbate, observed between -1.38 V and -1.58 V on the polarization curves (Fig. 3), on the charge transfer resistance (Fig. 5) and on the electrode capacitance (Fig. 6). It can be conceived that the electrode destabilization, which has been previously shown [7] to correspond to a progressive increase, with time, in the current minimum near -1.48 V, is considerably delayed due to the absorption of additive molecules which competes with the accumulation of the Ni/Zn-containing adsorbate.

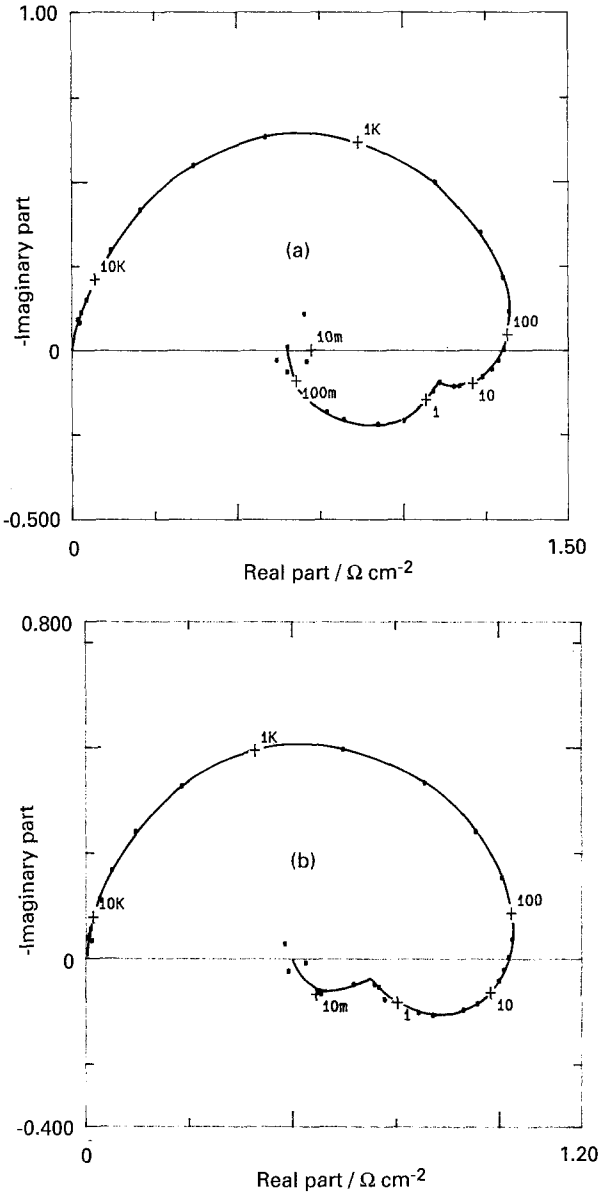

Fig. 8. Complex plane impedance plots recorded during galvanostatic zinc deposition ($i = 50\,mA\,cm^{-2}$), in the presence of $0.6\,g\,dm^{-3}$ TEBA. Deposition time: (a) 6.5 h, $E = -1.550$ V; (b) 60 h, $E = -1.526$ V.

4. Conclusion

The influence of an organic additive, triethyl-benzyl-ammonium chloride, on the mechanism of zinc deposition and reverse dissolution of zinc deposits in acidic sulphate medium, has been analysed. In the presence of Ni^{2+} ions it can be concluded that additive adsorption:

(i) inhibits the reaction of zinc deposition, first at the stage of nucleation and then during the growth of zinc deposits;
(ii) inhibits the hydrogen evolution taking place on a Ni/Zn-containing surface compound;
(iii) increases the charge transfer resistance and decreases the double layer capacitance over a wide potential domain (-1.38 to -1.58 V);
(iv) modifies the low-frequency impedance by magnifying the variation of the number of active sites for zinc deposition with increasing electrode polarization;

(v) stabilizes the galvanostatic deposition of zinc by competing with the formation of the Ni/Zn-containing adsorbate.

References

[1] R. C. Villas Boas, Synergetic phenomena in zinc electrowinning, NSF/SNPq, Rio de Janeiro, Brazil (1977).
[2] M. Maja, N. Penazzi, R. Fratesi and G. Roventi, *J. Electrochem. Soc.* **129** (1982) 2695.
[3] T. J. O'Keefe, S. F. Chen, E. R. Cole Jr and M. Dattilo, *J. Appl. Electrochem.* **16** (1986) 913.
[4] Y. M. Wang, T. J. O'Keefe and W. J. James, *J. Electrochem. Soc.* **127** (1980) 2589.
[5] D. J. Mackinnon and J. M. Brannen, *J. Appl. Electrochem.* **16** (1986) 127.
[6] S. Rashkov, M. Petrova and C. Bozhkov, *ibid.* **20** (1990) 11, 17.
[7] C. Cachet and R. Wiart, *J. Appl. Electrochem.* **20** (1990) 1009.
[8] *Idem*, The Electrochemical Society, 182nd Meeting, Toronto, Canada, Oct. 11–16 (1992). Extended Abstracts Vol. 92–2, p. 544. Also *J. Electrochem. Soc.* **141** (1994) 131.
[9] C. Cachet, R. Wiart, I. Ivanov and S. Rashkov, *J. Appl. Electrochem.* **23** (1993) 1011.
[10] D. J. Mackinnon, R. M. Morrison, J. E. Mouland and P. E. Warren, *ibid.* **21** (1991) 213.
[11] D. J. Mackinnon and J. M. Brannen, *ibid.* **12** (1982) 21.
[12] M. Sider and D. L. Piron, *ibid.* **18** (1988) 54.
[13] M. Sanchez Cruz, F. Alonso and J. M. Palacios, *ibid.* **20** (1990) 611.
[14] R. Wiart, C. Cachet, C. Bozhkov and S. Rashkov, *ibid.* **20** (1990) 381.
[15] C. Bozhkov, M. Petrova, I. Ivanov and S. Rashkov, Proceedings of the 7th European Symposium on Corrosion Inhibitors, *Ann. Univ. Ferrara NS* **9** (1990) 1211.
[16] C. Bozhkov, I. Ivanov and S. Rashkov, *J. Appl. Electrochem.* **20** (1990) 447.
[17] C. Cachet, R. Wiart, I. Ivanov and S. Rashkov, Microsymposium on Electrode Impedance Spectroscopy, Varna, May (1993), to appear in Communications of the Department of Chemistry, Bulgarian Academy of Sciences.